Original Research Article

Duckling lameness provides insight into osteoclast biology-I. Cytology

ABSTRACT Large multinuclear cells, osteoclasts (**OC**) were detected in bone marrow (**BM**) touch preparation smears by light microscopy using Wright-Giemsa stain. They are from femur samples of lame ducklings between 7 and 29d. OCs were found in BM proper, in areas populated mostly by erythroid and granulocytic developmental stages. These are located far from their usual place *in situ* (Howship's lacunae) as a component of the basic multicellular unit (**BMU**). Thus, they are called *ex situ* types.

Many are giants containing up to 50 nuclei of varying sizes. A single OC could contain a few small nuclei with areas ($\mathbf{A_N}$ ~ 30 μm^2) presumed as standard diploid types (2C). However, a majority of the nuclei are larger (A_N >1.6 x 30 μm^2) polyploids and aneuploid types. Nuclei may be located in restricted places (polarized) or uniformly distributed throughout the cytoplasm. Each nucleus contained up to 3 nucleoli themselves of varying size. The OC cytoplasm contains magenta or scarlet-colored "specific granules", presumably representing tartrate resistant acid phosphatase (TRAP), and (transcytotic) vacuoles; both characteristics of secretory cells. Examples of phagocytic types, faint nuclear types, and anuclear types were detected in the same preparation. In some instances, the OC showed signs of nuclear degradation and cytoplasmic fractures (necrosis). Interestingly, some OC contained engulfed cells appearing normal and were not apoptotic. These are likely examples of emperipolesis. Other engulfed cells showed signs of deterioration due to phagocytosis. It is not yet known if these OC cells represent escapees from the BMU or are formed Locally by the fusion of precursors. It is unknown if such cells are

homeostatic or pathologic but based on their peculiar cytology the latter seems more likely. These observations are the first report.

Key Words: osteoclast, bone marrow, duckling, cytology, lameness, giant cell

Abbreviations: A_C, cell area; A_N, nucleus area; BM**,** bone marrow**;** nm, nuclear membrane; Nx, number of nuclei; OC, osteoclast; P_C, cell perimeter; PR, ploidy ratio

1. INTRODUCTION

Osteoclasts (**OC**) are multinucleated cells responsible for bone resorption and remodeling. In human bone marrow (**BM**) they are rare, occurring at 2-3 cells per uL (Miyamoto and Suda, 2003). OC of chicken BM, from the embryo to the adult stage, are at <1% (Table 1; Lucas and Jamroz, 1961).

Experimental evidence indicates they derive from the fusion of mononuclear precursors in hemopoietic tissues. In the mouse system monocytes from BM, spleen and peripheral blood differentiate into OC by treatment with **RANKL** (receptor nuclear factor, **NF-Kb**) a member of the tumor necrosis factor (**TNF**) superfamily, and **M-CSF** a macrophage growth factor (Xu and Teitelbaum, 2013).

OC bone resorption is accomplished by matrix proteolysis. Homeostasis of Ca, hematopoiesis, and bone healing are also OC functions. Recent investigations expand OC functionality and place it as a member of the immune cell community. Their role in modulating immune suppression or inflammation is the subject of osteoimmunity, a growing field of interest (Madel, 2019). Removal of apoptotic cells by phagocytosis and regulation of self-tolerance by an OC are also important immune functions. Pathological conditions leading to inflammation are OC

associated (reviewed in Zupan et al. 2013). Collectively, cross-talk between OC and other immune cells is now well documented. The role of the OC in various bone diseases has been established experimentally with mouse models using genetic knock-outs; however, few observations on OC biology in non-mutation model systems are available (Guillemin, et al. 1995).

Traditional assumptions on OC life history have been challenged recently as the result of molecular and parabiosis studies (reviewed in McDonald et al., 2021). Now it is believed that OC life cycles are longer than traditionally thought and that they recycle.

Here the purpose is to explore the array of OCs of bone marrow samples from lame ducklings where other forms of atypia were also found (Cotter, 2021). These unusual cells may shed light on how an OC interacts with inflammatory cells of other series. Their description should contribute to a better understanding of the complexities of bone pathologies in avian food species where lameness is an important issue.

2. MATERIALS and METHODS

2.1 Ducklings

Ducklings ranging in age from 1 to 29 days were sampled at 2 commercial farms. All were grown on floor pens covered with wood shavings. A total of 9 lame ducklings were identified by experienced field service personnel who prepared the sample slides on site. Selected ducklings were removed from flocks in order to prevent further harm.

2.2 Welfare

Ducking welfare is monitored under the Maple Leaf Farms Trident Stewardship Program for Duck Well Being and procedures were reviewed by a PAACO certified auditor and licensed Veterinarian.

2.3 Sample Collection

Companion touch preparation slides were made at each farm site from femur bone marrow (**BM**) and blood. Specimens were spread across clean glass microscope slides and immediately air-dried. Once dried, slides were immersed in 95% ethanol and postfixed for 10 to 15 min. Slides were stained by Wright's method followed by a brief exposure to Giemsa using an in-house procedure (Cotter, 2021).

2.4 Light Microscopy and Photomicrographs

Olympus CX-41(Olympus America, Center Valley, PA 18034-0610) equipped with Plan N 40x, 0.65 numerical aperture dry, and Plan N, 1.25 numerical aperture 100x oil objectives. All images were captured at 100x with an Infinity-2 1.4-megapixel charge-coupled device Universal Serial Bus 2.0 Camera, and processed with Infinity Analyze software (Release 6.5) (Lumenera, Inc., Ottawa, ON, Canada).

2.5 Ploidy Ratio (PR)

Ploidy is estimated by the division of nuclei areas (A_N) by the area of the smallest (reference) nucleus (A_R, ~ 30 μm^2), assumed as representing the diploid condition (2C). A PR value of $\geq$ 1.6, as used for flat plant cells (Melaragno et al.,1993) indicates a polyploid nucleus. Thus PR = A_N/A_R.

3. RESULTS

In lame ducklings, OCs were found in medullary BM, distant from Howship's lacunae. These *ex situ* types are the present subject. Thirty-four *ex situ* OCs were located by scanning at

40x magnification across a BM touch-preparation smear obtained from a 13d lame duckling. An average OC has a perimeter ($\mathbf{P_C}$) of 213 (+/- 8) μm, with an area (A_C) of 2438 (+/- 201) μm^2. Nuclei number averaged 12.4 (+/- 2); ranging between 0 to 50. OCs were subclassified as faint nuclei types (N = 18) phagocytic (N = 9) anuclear (N = 3) necrotic (N = 1) micronuclei (N =1) and not further classified (N = 2).

The cells chosen for description are selected to indicate the diversity of OC cytology; all were located on the same slide taken from a 13d lame duckling. The presentation begins with a model type and proceeds to examples of other types.

3.1 Model ex situ OC

Insert figure 1 here

Figure 1 is a model OC; the cell is large [A_C 2213 μm^2] multinuclear [N = 11] with nuclei restricted to one hemisphere (polarized). The cytoplasm is differentiated into basophilic endoplasmic and clearer ectoplasmic areas. It contains "specific" granules (scarlet) and clear vacuoles; concentrated in the ectoplasm. The nuclei have 1 or 2 nucleoli and the nm is intact. Nuclei area (A_N) range from 43 -72 μm^2 [Ave 56 μm^2 +/- 9.0]. The nuclear PRs range from 1.4 - 2.4 [Ave 1.9] indicating that nearly all are polyploid. The number of nucleoli seen within individual nuclei support polyploidy. The OC is in a BM area predominated by erythroid developmental cells and atypical (necrotic granulocytes). A few eosinophils, uncommon in circulating blood, are in the field. One of which (11 o'clock) seems to be entering (emperipolesis) the cytoplasmic domain of the OC. A partially degraded RBC (9 o'clock) with cell-associated bacteria (CAB) has been phagocytosed (arrows).

3.2 Phagocytic/emperipolesis OC

Insert Figure 2 here

A phagocytic OC is found in a bed of developmental and mature RBC scattered among a few developmental granulocytes and mature cells. It has 11 nuclei and contains a phagocytosed heterophil (H) whose remnants are at 3 o'clock. A small lymphocyte (Ls) is also internalized by the OC by emperipolesis and remains intact. The Ls cm has 2 blebs seen projecting from opposite poles. The large OC nuclei range from 36 μm^2 (diploid) to 85 μm^2 (hexaploid, *) and contain from 1 to 3 nucleoli. A few specific granules and vacuoles are seen scattered at the OC edge.

3.3 Faint Nuclei OC

Insert figure 3 here

A giant OC [A_C 4201 μm^2; P_C 262 µm] in which most nuclei have deteriorated is in Figure 3. The remaining intact nuclei are near the arrow at the top right; one [A_N 61 μm^2] is likely tetraploid. The central endoplasm is notably basophilic and contrasts with a broad band of clearer ectoplasm. A few specific granules of varying size are clustered at the right (3 o'clock) and many smaller types are at the bottom edge (6 o'clock) of the mother cell. A partially degraded RBC at the lower left is adjacent to a phagocytic vacuole (*) containing remnant cytoplasm of uncertain origin.

3.4 Necrotic OC

Insert figure 4 here

Figure 4 shows a giant [A_C ~ 3280 μm^2; P_C ~323 µm] necrotic multinuclear OC (~20N) of irregular shape. It resides in an area loosely populated by erythroid and granulocytic developmental cells. Most nuclei are barely visible. The mother cell appears to be in a process of

separation into smaller cytoplasmic masses. There is an obvious fracture of the cytoplasm running across the equator.

3.5 Micronuclei OC

Insert Figure 5 here

An example of a giant OC (A_C ~2406 μm^2; P_C ~227 μm) was seen in a lame 13d duckling form in which *Streptococcus sp.* were isolated. It is a type with multiple small faint nuclei (Figure 5). Only 5 nuclei located at the left edge were able to be measured. These gave an average area (A_N) of ~ 16.1(+/- 0.15) μm^2. These areas are ~ half that of diploid types. Thus, they are called "micronuclei." The remaining nuclei were too faint to be measured accurately. The OC was phagocytic having engulfed several RBCs, and a developmental cell likely a member of the erythroid series has entered its cytoplasm by emperipolesis. The cm is irregular and diffusely organized, particularly on the right side; rendering both the A_C and P_C measurements somewhat uncertain. Although a few of the neighboring cells show signs of necrosis (faint staining) the OC itself appears further along a necrotic pathway than the majority of its neighbors. This raises the possibility that this OC represents a necrotic nidus; a source of diffusible toxins affecting the neighboring community.

3.6 Anuclear OC

Insert figure 6 here

Figure 6 is an anuclear OC [Ac 2149 μm^2; Pc 191 μm] located in an area of BM populated mostly by cells of the erythroid series. Definitive nuclei were not observed but the cytoplasm appears to contain suggestions of remnant nuclei; one is circled. Specific granules are dispersed

throughout; vacuoles are not seen. The main cytoplasmic mass is surrounded by a clear zone possibly representing traces of former ectoplasm.

3.7 Supergiant Polynucleated OC

Insert figure 7 here

Figure 7 is an elongated supergiant OC located in an area of BM thinly populated with cells of the erythroid series (Ac 3313 μm^2; Pc 239 μm). N1 is used as a reference nucleus (diploid, $A_R \sim 30\ \mu m^2$) and N17 is tetraploid ($A_{N17} \sim 60\ \mu m^2$). Nuclei contained up to 3 nucleoli. A degraded nucleus is located by the arrowhead.

3.8 Ploidy Study

Ploidy was studied by measuring the sizes of 18 nuclei in the supergiant OC of Figure 7. The PRs for each nucleus were determined by the division of the area of a given nucleus by the area of the smallest nucleus, A_N/A_R (Figure 8). The cut-off PR 1.6 is a value used for flat (plant) cells (Melaragno et al., 1993). This seems value appropriate for *ex situ* OC's because they are also flat cells. The vertical reference lines represent the locations of empirically determined inflection points marking the separations of diploid, aneuploid (2N+), triploid, and higher ploidy nuclei respectively. The 5 nuclei to the left of the first vertical reference (28%) are the smallest nuclei and so represent diploids (2N); the 2 to the right of the >4N reference line are the largest and are at least hexaploid. The nuclei occupying the central area represent various aneuploid (2C+/2N+) types. Micronuclei (Figure 5; $A_N \sim 16\ \mu m^2$) are likely < 2C/2N and are not considered by Figure 8.

Insert Table 1 here

4. DISCUSSION

The present observations expand the basic information currently available on the avian OC. The traditional remodeling view of the OC applies to the resorption of bone by a cell located in a Howship's lacunae, as a component of the BMU (Gay, et al. 1993). Here it is demonstrated that the OC can also be found in medullary BM. These *ex situ* types appear to share certain characteristics with their *in situ* counterparts. They are multinuclear, often with a polarized nuclear distribution characteristic of BMU types. They possess specific cytoplasmic granules and (transcytotic) vacuoles both characteristics of secretory cells. However, in contrast, they are much larger, more irregularly shaped, and contain many more nuclei than the 6-8 typical of *in situ* types (Guilleman, et al 1995).

Some *ex situ* types are obviously phagocytic as demonstrated by the examples in Figures 2 and 3. Moreover, they can accommodate eosinophils and erythroid cells by emperipolesis. Furthermore, some of the nuclei of *ex situ* types are not stable and prone to disintegration as is the case for the nuclei of cells in Figures 4, 5, & 6. Loss of nuclear functionality can result in a near anuclear mass of cytoplasm still retaining some features of an intact OC (Figure 6). In other cases, the partially anuclear mass can undergo fragmentation (Figure 3).

Nuclei of *ex situ* OC deserve special attention. Unlike their *in situ* counterparts, their number often exceeds the (6-8) seen in standard avian types. Not only are the *ex situ* nuclei higher in number than standard types but most are polyploid (Figures 7, 8). Generally, these are signs of increased metabolic (resorptive?) capacity. Presumably, these giant cells form by fusion of (diploid?) mononuclear precursors. However, both questions will require additional study.

The author is aware that the application of a (1.6) size cut-off to determine ploidy, a principle established for flat *Arabidopsis* cells (Melaragno, et al 1993) is open to debate. Future investigations may necessitate its modification.

It is clear from the current observations that OCs express overlapping properties; phagocytosis and emperipolesis are examples, so separating into subcategories is a convenience rather than a biological distinction. It is also obvious that some OCs appear to be pathogenic while others might benefit the host; especially by phagocytosis and removal of pathogens or necrotic cells of another series.

Many questions regarding these OCs remain unanswered. What is their origin? Are they escapees from the BMU? If so, why do they have so many nuclei? If they are not escapees, how are they formed? The standard OC is polyploid due to the fusion of monocytic precursors with diploid nuclei. OCs might be described as polykaryons; multiple 2N nuclei housed in a common cytoplasm. However, recently it has been shown that some OC polyploidization in the mouse system results from incomplete cytokinesis; nuclear division without cytoplasmic separation (Takegahara, et al 2016). This observation is supported by the small size of the nuclei seen in Figure 5 and the nuclear size distribution in Figure 8. This suggests *ex situ* types may result from several formation mechanisms. If *ex situ* types form by fusion, some precursor cells should be found having only one or a few (polyploid) nuclei. Are *ex situ* OCs beneficial or do they contribute to the development and progression of lameness because they exacerbate inflammation?

In situ OCs are highly polarized cells when in the bone resorptive phase (Väänänen and Horton, 1995). Some *ex situ* OCs retain this characteristic (Figures 1, 2, 3) others do not (Figures 4, 5).

How polarization of *ex situ* OCs pertains to a potential benefit or detriment of the host (Väänänen et al 2000) is under study.

5. CONCLUSION

In conclusion, the present observations constitute the first description of *ex situ* OC cell type(s) with multiple properties; in addition to those of standard *in situ* BMU types. Since these cells were seen in lame ducklings, they should attract the interest of a variety of investigators who specialize in bone disease. Some of the questions regarding OC biology raised by these cells as their formation and degradation mechanisms are currently under investigation.

REFERENCES

1. Miyamoto T, and T Suda, 2003. Differentiation and function of osteoclasts. The Keio Journal of Medicine, 52(1): 1–7. https://doi.org/10.2302/kjm.52.1

2. Lucas AM and C Jamroz, 1961. Atlas of Avian Hematology, Monograph 25 USDA, Washington

3. Xu F, and S Teitelbaum, 2013. Osteoclasts: New Insights. Bone Res 1: 11–26. https://doi.org/10.4248/BR201301003

4. Madel MB, L Ibáñez, W Abdelilah, et al. 2019. Immune function and diversity of osteoclasts in normal and pathological conditions. Frontiers in Immunology 10: 1408 URL=https://www.frontiersin.org/article/10.3389/fimmu.2019.01408 DOI=10.3389/fimmu.2019.01408

5. Zupan J, M Jeras, and J Marc, 2013. Osteoimmunology and the influence of pro-inflammatory cytokines on osteoclasts. Biochem Med (Zagreb) 23(1): 43–63. doi: 10.11613/BM.2013.007 PMCID: PMC3900089 PMID: 23457765

6. Guillemin G, SJ Hunter· and CV Gay, 1995. Resorption of natural calcium carbonate by avian osteoclasts in vitro. Cells and Materials 5 (2):157-165 Scanning Microscopy International, Chicago (AMF O'Hare), IL 60666 USA

7. McDonald MM, AS Kim, BS Mulholland, M Rauner, 2021.New insights into osteoclast biology. JBMR Plus.5(9):e10539. doi: 10.1002/jbm4.10539. PMID: 34532619; PMCID: PMC8441501.

8. Cotter PF, 2021. Atypical hemograms of the commercial duck. Poultry Science 100:101248 https://doi.org/10.1016/j.psj.2021.101248

9. Melaragno JE, B Mehrotra, AW Coleman, 1993. Relationship between endopolyploidy and cell size in epidermal tissue of Arabidopsis. Plant Cell 5(11):1661-1668. doi:10.1105/tpc.5.11.1661

10. Gay CV, NL Kief, PJ Bekker, 1993. Effect of estrogen on acidification in osteoclasts. Biochem Biophys Res Commun.192(3):1251-9. doi: 10.1006/bbrc.1993.1551. PMID: 8389545.

11. Takegahara N, H Kim, H Mizuno, et al., 2016. Involvement of receptor activator of nuclear factor-κb ligand (RANKL)-induced incomplete cytokinesis in the polyploidization of osteoclasts. The Journal of Biological Chemistry 291(7):3439-3454. DOI: 10.1074/jbc.m115.677427. PMID: 26670608; PMCID: PMC4751386

12. Väänänen HK, Horton M, 1995. The osteoclast clear zone is a specialized cell-extracellular matrix adhesion structure. J Cell Sci.108 (Pt 8):2729-32. doi: 10.1242/jcs.108.8.2729. PMID: 7593313.

13. Väänänen HK, Zhao H, Mulari M, Halleen JM, 2000. The cell biology of osteoclast function. J Cell Sci. (Pt 3):377-81. doi: 10.1242/jcs.113.3.377. PMID: 10639325.

DECLARATION

The author declares that the research was conducted in the absence of any commercial or financial relationships that could be construed as a potential conflict of interest.

Figure Legends:

Figure 1. A model *ex situ* OC is a large multinuclear cell with 12 polarized nuclei and with vacuolated cytoplasm containing specific granules. Cell associated bacteria are located with arrows. Additional descriptions are in the text.

.

Figure 2. A model phagocytic OC containing a small lymphocyte (Ls) that has entered by emperipolesis. Additional descriptions are in the text.

Figure 3. A giant phagocytic OC with many faint and intact nuclei. Additional descriptions are in the text.

Figure 4. A giant necrotic OC with an irregular shape. Additional descriptions are in the text.

Figure 5. An OC with micronuclei. Additional descriptions are in the text.

Figure 6. An anuclear OC. A nuclear remnant is circled. Additional descriptions are in the text.

Figure 7. An example of a polynucleated (N18) supergiant OC with a nuclear remnant (arrow). N1 is the reference nucleus ($A_N \sim 30\ \mu m^2$) and N17 ($A_N \sim 60\ \mu m^2$) is one of the largest sizes. Additional descriptions are in the text.

Figure 8. Scatter plot of ploidy ratios ($PR = A_N/A_R$) and ploidy cut-offs where $A_R \sim 30\ \mu m^2$

Figures

1.

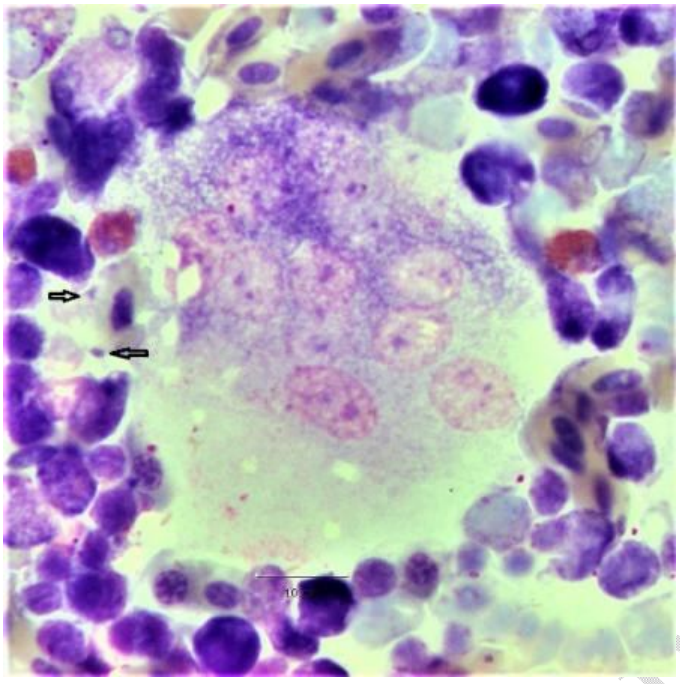

2.

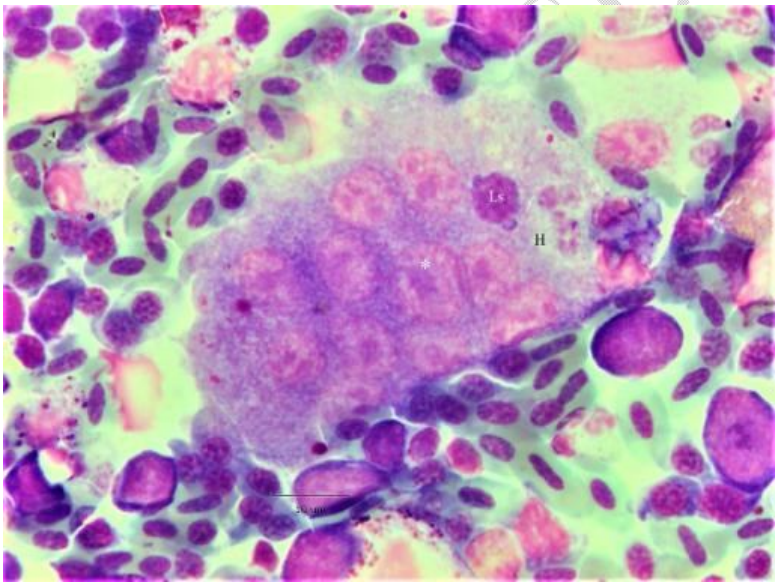

3.

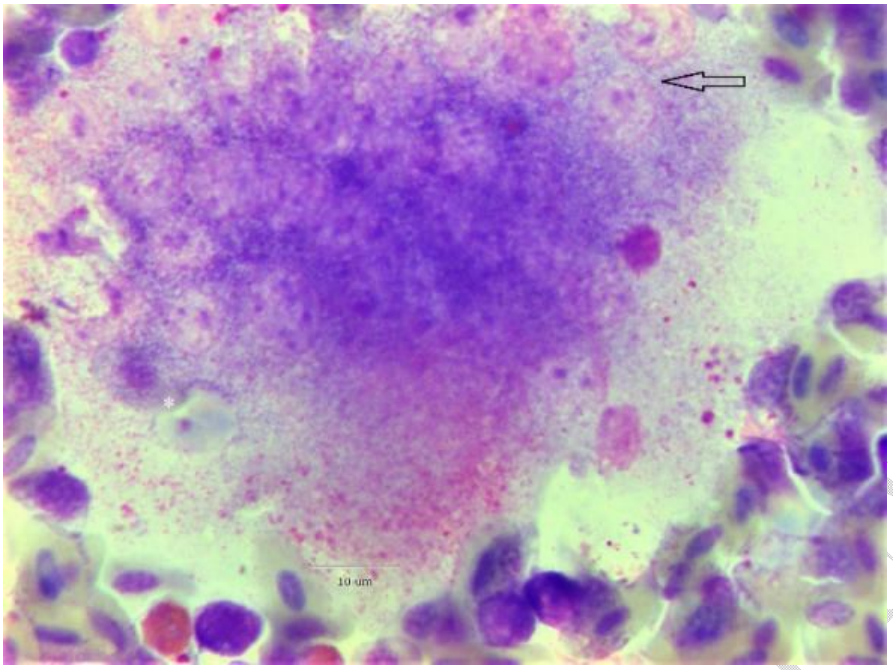

4.

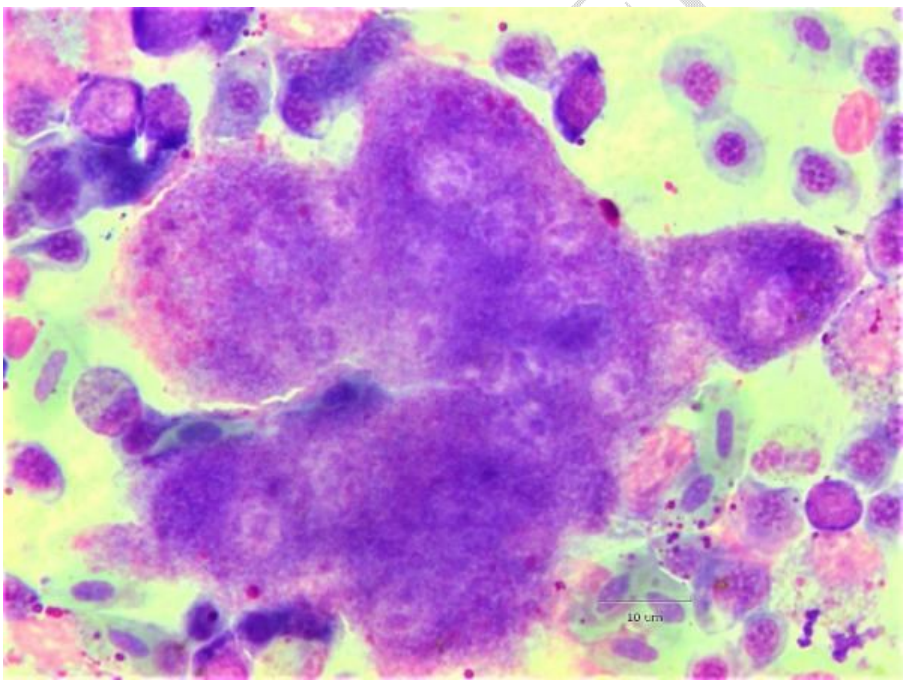

5.

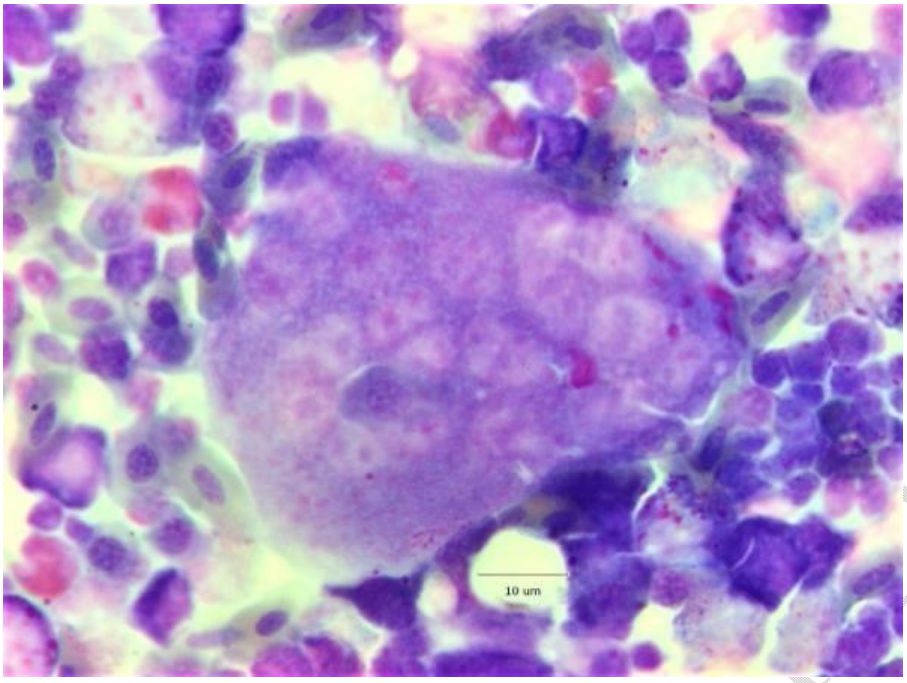

6.

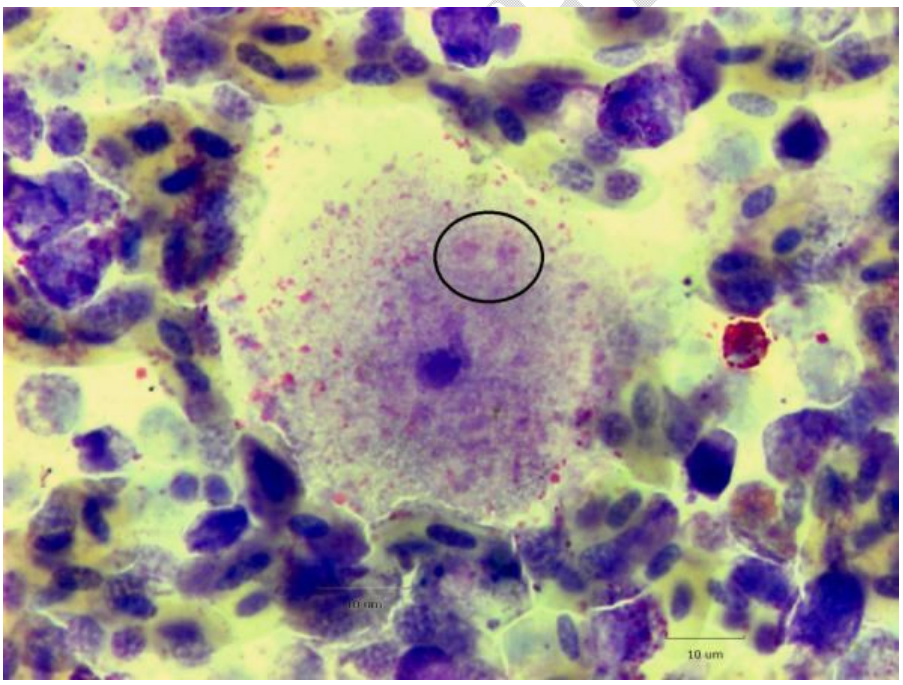

7.

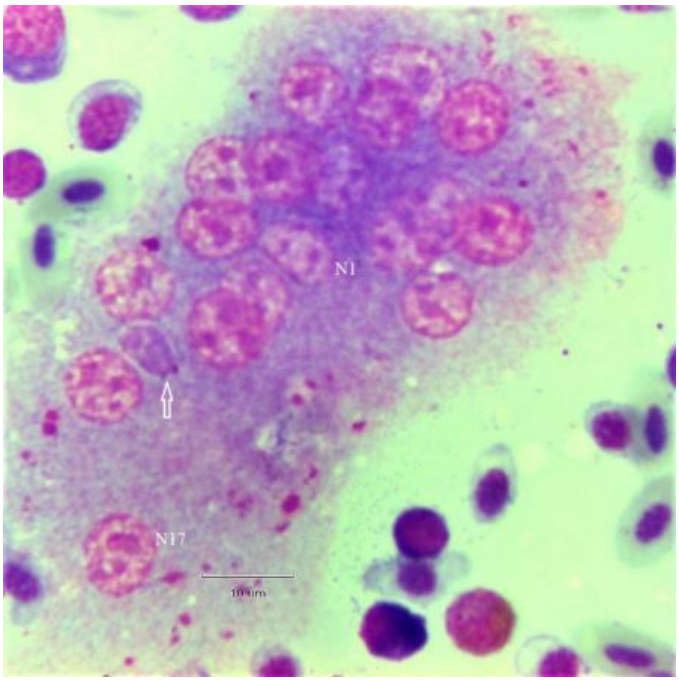

8.

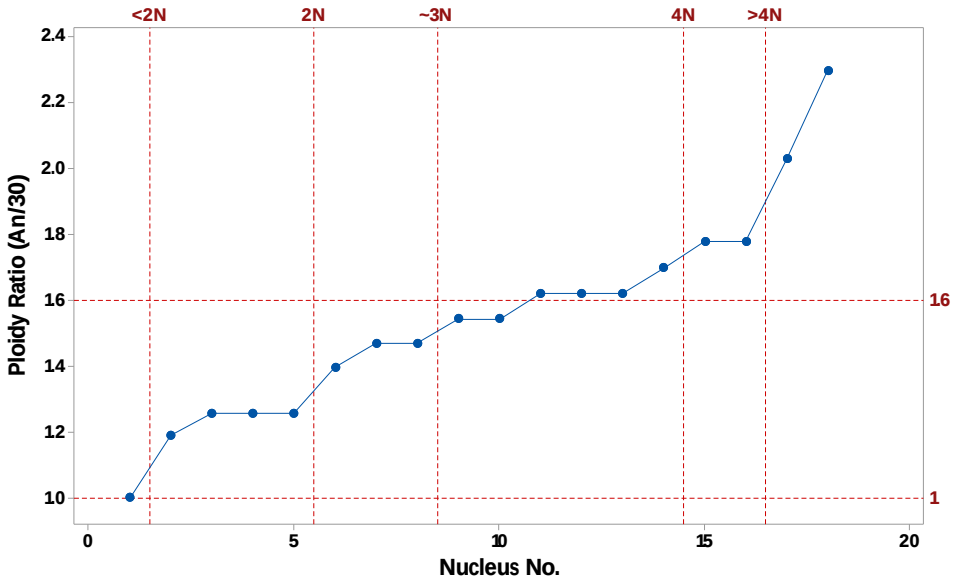

Figure 7 P/R Ratios

Table 1. Figure 7 average nuclei area (μm^2) and standard errors (SE) as classified by assumed ploidy.

Ploidy	N	Ave Area	SE
<2	1	34.2	-
2	4	42.4	0.6
3	9	53.1	1.1
4	2	60.8	0.0
>4	2	74.0	4.6